Toward Performance Specifications for Concrete Durability: Using the Formation Factor for Corrosion and Critical Saturation for Freeze-Thaw

W. Jason Weiss, PhD
Edwards Distinguished Professor of Engineering
Oregon State University, School of Civil and Construction Engineering,
111F Kearney Hall, Corvallis OR 97331
Tel: 541-737-1885; Email: jason.weiss@oregonstate.edu

M. Tyler Ley, PhD, PE (CA)
Associate Professor of Civil Engineering
207 Engineering South
Stillwater, OK 74075
Tel : 405-744-5257; Email: tyler.ley@okstate.edu

O. Burkan Isgor, PhD, PE (ON)
Professor
Oregon State University, School of Civil and Construction Engineering,
302 Owen Hall, Corvallis OR 97331
Tel: 541-737-3052; Email: burkan.isgor@oregonstate.edu

Thomas Van Dam, Ph.D., P.E. (IL, MI, NV)
Principal, NCE
1885 Arlington Ave., Suite 111
Reno, NV 89509
Tel: 775-527-0690; Email: tvandam@ncenet.com

Word count: 5993 words + 6 tables/figures (x 250 words each) 1500 = 7493 words

Submission Date July 30th, 2016

Toward Performance Specifications for Concrete Durability: Using the Formation Factor for Corrosion and Critical Saturation for Freeze-Thaw

Jason Weiss, Tyler Ley, Burkan Isgor, Tom Van Dam

Abstract

This paper discusses the development of a conceptual framework for the specification of concrete durability using performance modeling concepts. Specifically, the approach will relate acceptance tests, material properties, degradation models, limit states, and reliability. When implemented, this approach can be used for a variety of distress mechanisms; examples are provided for two specific distresses. In the first example, the formation factor is used to describe the transport of chloride ions that indicate the onset of depassivation and corrosion in a reinforced concrete element. In the second example, a sorption based model is presented to describe performance of concrete in a freeze-thaw environment. While the test methods will need to be refined and models will require further calibration based on rigorous evaluation and improvement in the coming years, this framework has great potential to directly relate measured concrete properties to the long term durability performance of concrete structures.

1.0 Review and Motivation for Performance Specifications

Construction specifications are a series of instructions provided by a state highway agency (SHA) to a contractor/producer (C/P) that describes the characteristics of the materials to be used and/or a process for performing work on a project. While specifications cover many aspects of construction, this paper focuses primarily on concrete as a material, providing a link between measurable aspects of concrete and anticipated performance of the concrete in a given environment. While the vast majority of concrete specifications have historically been prescriptive specifications, performance specifications are increasingly being discussed as one potential alternative (1). It is the position of the authors that an opportunity exists for specifications that address durability concepts through simple tests at the time of concrete placement or shortly thereafter that can be directly related to performance.

Performance based specifications can take many forms (1-12). Goodspeed et al. (3) developed a performance specification for high performance concrete by establishing performance grades based on eight standard tests. Ozyilidirim (4) discussed the development of quantitative relationships linking tests to performance. NRMCA developed performance based standards that relate hardened concrete requirements to established testing criteria (2). Performance Related Specifications (PRS) have also been developed in the late 1990s for pavements (5,6,7,8) that link tests, performance and repair costs. While not a specification per se, The International Federation for Structural Concrete (fib) has developed a model code that outlines calculations of several durability related distresses (9), as have others (10,11,12).

This paper is written as PRS specifications software is currently being updated to include, among other advancements, increased attention to durability (13). Similarly, an expert task group (ETG) has been developed to look at performance engineered mixtures (14). This paper discusses an approach that could be used for PRS for concrete materials used in pavements, bridge decks, and other concrete applications.

The basic concept of a performance specification, as presented herein, is to develop quantifiable relationships between the materials used, exposure conditions, and anticipated life and costs of the concrete. The basic framework for the performance specification consists of several steps outlined in Figure 1 (12,15). In Step 1, standardized material tests are performed to evaluate the materials being used. These tests can be used either to qualify the mixture, accept the mixture, or both. While some tests have been used historically, it is anticipated that the concrete community will need to become familiar with new tests. The results of these standardized tests are used in Step 2 to obtain the fundamental material properties needed in service life models to assess long term durability. In Step 3, the material properties (from step 2) are used in models to evaluate a specific deterioration mechanism (e.g., the chloride ingress in concrete) and to evaluate the time it takes to reach a specific limit state in an particular environment (e.g., ions on a bridge deck reaching a critical concentration at the depth of the reinforcing steel). Finally, the results of the individual models are quantified using reliability in terms of anticipated service life (e.g., 30 years) or a probability of a limit state occurring (e.g., less than 10% probability of corrosion). Reliability can be accounted for using a statistically-based approach (15) to quantify the probability of reaching a limit state.

The transport processes used in this paper for corrosion will rely on the formation factor. The formation factor can be related to a wide variety of transport properties and can be used to address a wide range of durability problems (e.g., alkali silica reactivity, sulfate damage, freeze-thaw). The formation factor can be easily specified and compliance with the specification can be determined with rapid electrical resistivity measurements. While this paper focuses specifically on chloride transport and the onset of the corrosion of reinforcing steel, other applications for the formation factor can also be shown.

While the approach described in this paper provides a framework, there is no doubt that test methods, models, environmental factors, and variability distributions will need extensive development, calibration, and will be improved upon in the coming years. Further, this approach can be extended to include a variety of degradation modes and more sophisticated models over time. *In other words, this paper provides a framework for clear path forward that can provide practical results today, as well as be expanded for increased use in the future.* This approach also enables local exposure conditions to be included so that the specification is 'tailored' unique environmental and site conditions. It is noted that the models used in this approach are 'comparative' in that they enable a relative comparison between conditions; as such, they do not

imply an absolute relationship to field performance and relationships with in-service performance will develop over time and with model calibration and modification.

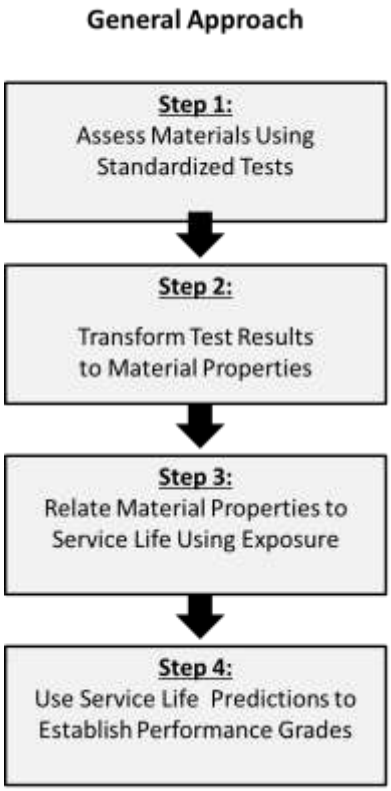

Figure 1: Approach to use performance models in performance specification development (after 12,15).

The next section of the paper provides two examples to illustrate how this framework can be applied to challenging durability problems facing SHAs.

3. Example 1: Specifying a Formation Factor to Assess the Corrosion of Reinforcing Steel in a Concrete Bridge Deck

3.1 Relating the Formation Factor to Exposure to Determine the Time to Corrosion Initiation

While electrically-based test methods for concrete have been used for approximately a century (16,17,18), the last decade has seen major advancements in the development of electrical tests to rapidly and accurately assess the properties of field concrete (19,20,21). The formation factor can be obtained from electrical resistivity and is a fundamental property that can be used to describe the rate of ionic diffusion and the onset of steel depassivation and corrosion in reinforced concrete elements. Figure 2 illustrates how a standardized test for electrical resistivity can be related to the formation factor. Details on how to obtain the formation factor from electrical resistivity testing is provided in section 3.3.

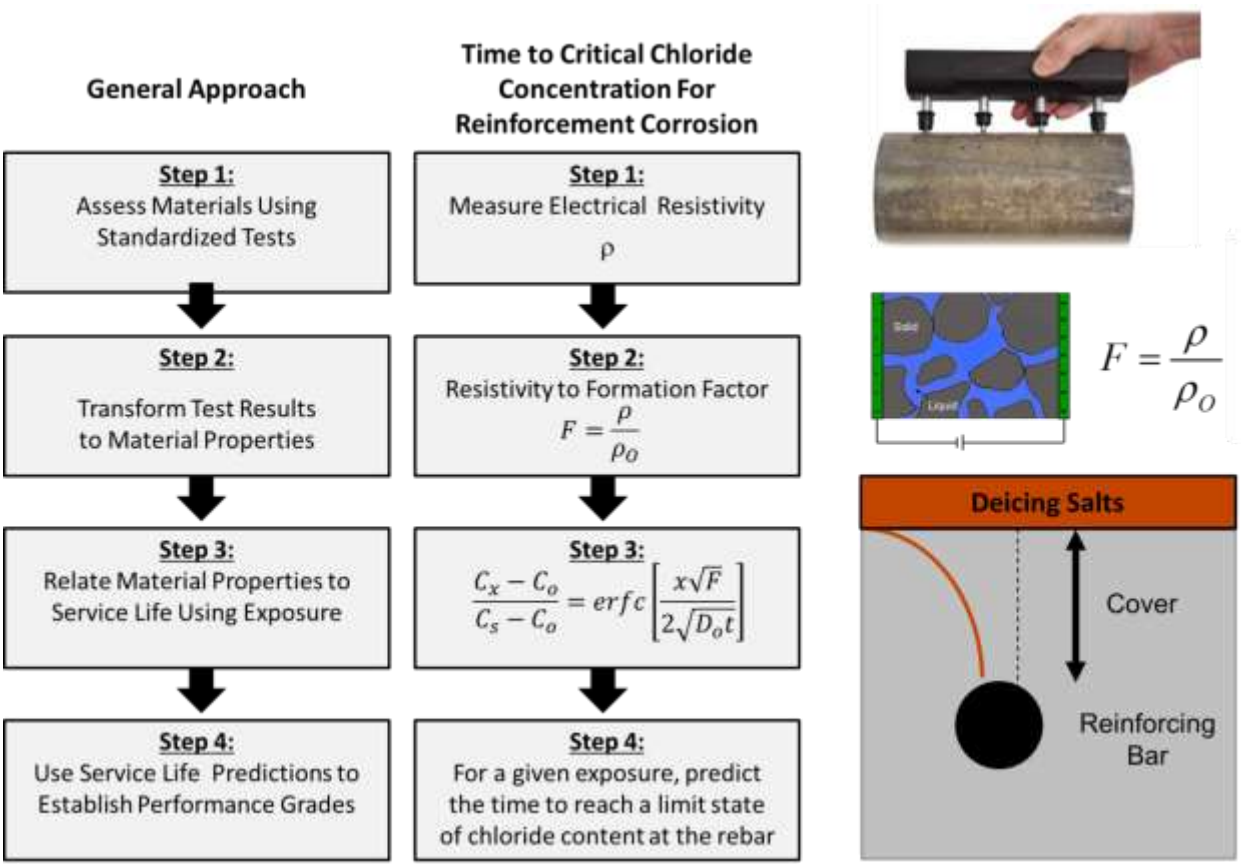

Figure 2: Extending the performance model approach to corrosion of reinforcing steel in bridge decks

To begin, consider a concrete section with a reinforcing bar that is placed at a distance x from the concrete surface (Figure 2). At the surface of the concrete section salt is present from an exposure to deicing salts or seawater. For a one-dimensional ingress problem, the corrosion process is frequently modeled using a simplified diffusion-type process which can be represented by the error function solution of the Fick's second law shown in equation 1 (22).

$$\frac{C - C_o}{C_s - C_o} = 1 - erf\left[\frac{x}{2\sqrt{Dt}}\right] \qquad \text{Equation 1}$$

where C_S is surface salt concentration, Co is the original chloride concentration, C is the chloride concentration, D is a diffusion coefficient, and t is time. When C exceeds the chloride threshold at the depth of the reinforcing steel (noted as Cx, for the analyzed steel-concrete system) depassivation occurs, corrosion begins, and t represents the time to corrosion initiation (or depassivation). To determine the life of a reinforced concrete element before repair is needed, it is common to add a time for the propagation of corrosion to the time to the depassivation time. While determining the propagation time is still an active area of research (23,24), it is common in service life models to assume a propagation time (e.g., 6 years) (22).

The diffusion coefficient D can be related to the formation factor, and therefore to the electrical resistivity using Equation 2:

$$D = \frac{D_o}{F} = \frac{D_o \rho_o}{\rho_{Concrete}} \qquad \text{Equation 2}$$

where D_o is the self-diffusion coefficient for a chloride ion (2.03×10^{-9} m^2/sec at 25°C) and ρ_o is the pore solution resistivity (the determination of pore solution resistivity described in more detail in section 3.2).

Substituting the formation factor from equation 2 into equation 1 yields equation 3

$$\frac{C_x - C_o}{C_s - C_o} = 1 - erf\left[\frac{x}{2\sqrt{\left(\frac{D_o}{F}\right)t}}\right] \qquad \text{Equation 3}$$

Equation 3 can be rearranged so that the formation factor can be directly related to the time of corrosion (t) for a given environmental exposure (C_S) and cover thickness (x).

$$F = \frac{4tD_0}{x^2}\left[erf^{-1}\left[\frac{C_s - C_x}{C_s - C_o}\right]\right]^2 \qquad \text{Equation 4}$$

Figure 3 illustrates the relationship between the formation factor and the time to corrosion for concrete (assuming 62.5 mm cover, surface concentration (C_S) of 0.7% of the mass of concrete, a chloride threshold (C_X) of 0.15% of the mass of concrete, and an initial chloride concentration (C_O) of 0% of the mass of concrete. Fick's second law is a reasonable approach however this formulation assumes that no chloride binding occurs with aluminates or other phases in the hydrated cementitious matrix. This will be discussed later in this section.

Figure 3a illustrates that a formation factor of 1190 or greater would be needed (ignoring uncertainties and variability) to provide a concrete element with a 62.5 mm cover with a life of 30 years (24 years to depassivation plus 6 years of propagation) before repair would be needed using the exposure condition described above. The impact of varying the cover thickness is also shown in Figure 3a. The time to depassivation is related to the square of cover thickness, as it can be observed from equations 4.

Variability in chloride loading can be considered using Monte Carlo techniques assuming a normal distribution with a coefficient of variation for C_S of 10%, a coefficient of variation in

the cover thickness of 30%, and a coefficient of variation in F of 20%. Figure 3b illustrates the impact variability on the time to repair by assuming each line represents the statistically determined proportion of elements requiring repair for a given formation factor (mean C_S = 0.7% of mass of concrete, mean x= 62.5 mm). For example, the 20% line (shown with open circles) denotes the relationship between the formation factor and the time that 20% of the elements would need to be repaired (19 years). The exposure conditions and variabilities have been selected for illustrative purposes and would need to be refined for a given location.

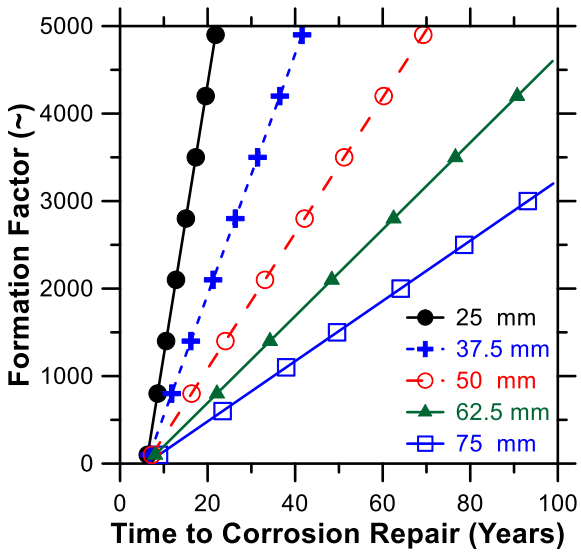

(a)

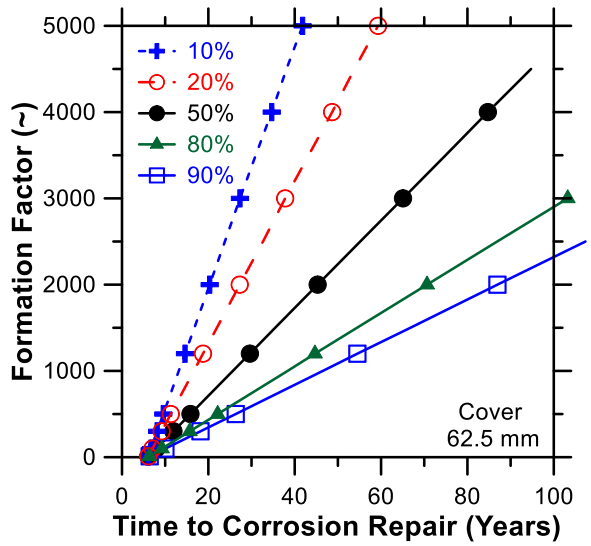

(b)

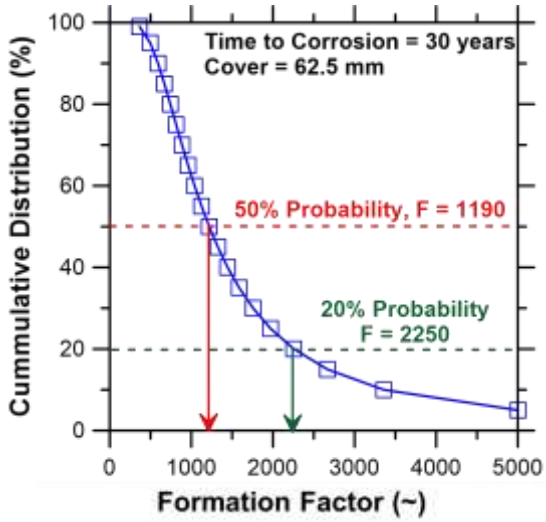

(c)

Figure 3: Predicted time to corrosion: a) influence of cover thickness, b) variability in the percentage of elements requiring repair, c) variability in time to corrosion for a time to repair of 30 years.

Figure 3c illustrates the probability distribution associated with the formation factor required for a time to repair of 30 years with different levels of confidence (reliability). While a formation factor of 1190 is required for 50% of the elements to survive for 30 years without needing repair, the F Factor of 2250 is required for 80% of the elements to survive for 30 years without needing repair.

It should be noted that equations 1 to 4 illustrate the concept of how the formation factor can be used. These results do not consider temperature effects or concrete aging however these factors could easily be included in the formulation. Further, equations 1 to 4 do not consider chloride binding. There are different ways of incorporating binding (25,26); however, a commonly used approach is to use an apparent diffusion coefficient as shown in equation 5 (27).

$$D_{App} = \frac{D}{1+\frac{\partial C_B}{\partial C}} = \frac{D_o}{\left(1+\frac{\partial C_B}{C}\right)F} \qquad \text{Equation 5}$$

where C_B and C are the concentrations of bound and free chlorides using empirically determined chloride binding isotherms (27,28). Typically chloride binding can be described using a Langmuir isotherm where α and β are empirically determined (27):

$$\frac{\partial C_B}{\partial C} = \frac{\alpha}{(1+\beta C)^2} \qquad \text{Equation 6}$$

Substituting D_{App} into equation 1 (in place of D) results in the need to use a numerical scheme such as finite difference or finite element method to obtain a solution. Here, the problem is solved deterministically using a finite element method for three cases: 1) without binding, 2) with a low level of binding (α = 1.67; β = 0.12), and 3) with a high level of binding (α = 1.67; β = 0.04). Figure 4 illustrates that the use of the formation factor without binding is the most conservative time to corrosion while low and high binding cases provide times to corrosion that are approximately 14% and 60% greater than the no binding case, respectively (Figure 4a).

While it may immediately appear that binding makes a large difference in the results and would need to be considered in all simulations, it should be noted that binding also impacts the surface chloride concertation, C_S. For the simulations shown in Figure 4a the surface concentration for the no binding case used 0.70% of the mass of concrete for all simulations. This would result in a non-bound (free) chloride concentration of 0.7% by mass of concrete at the surface for the case without binding and a surface concentration of 0.44% of the mass of concrete for the high binding case. In reality however the C_S value will vary for different environmental exposure and for a C_S of 0.70% by mass of concrete for no binding the equivalent C_S would be 1.08 for high binding (as determined from the binding isotherm)). When binding and its impact on surface loading are considered together (Figure 4b), the average predicted time to corrosion was 7% greater for the case with binding (assuming the higher F associated with

binding along with the greater surface concentration, C_S). This indicates that the time to corrosion is similar for different levels of binding than initially assumed using only Figure 4a.

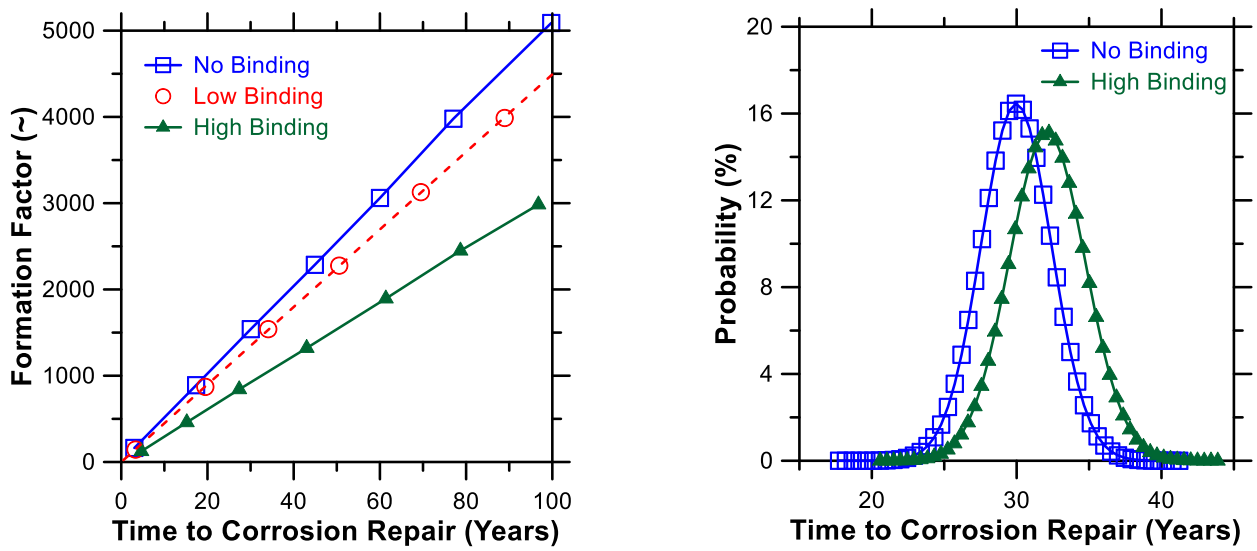

(a) *(b)*

Figure 4: Predicted time to corrosion illustrating the influence of binding

3.2 Relating the Formation Factor to Electrial Resistivity (Step 2)

While the previous section has illustrated how the formation factor is a fundamental property that can be related to the time to corrosion, this section will show how the formation factor can be determined using electrical testing methods. The use of electrical test methods has substantially increased in the last decade with advancements in the portability and measurement speed of hand-held testing devices and adoption for use by a number of SHA (19,29,30). Electrical measurements are an attractive test method due to their ease of use, ability to be performed rapidly, and the low cost of the testing equipment (19).

The formation factor can be used to characterize the pore structure of concrete since it is dependent on the pore geometry and connectivity. The formation factor is defined as the ratio of the resistivity of a bulk body and the resistivity of the pore solution in the body (ρ_o), as shown in equation 7.

$$F = \frac{\rho\ [\Omega \cdot m]}{\rho_o\ [\Omega \cdot m]} \qquad \text{Equation 7}$$

The pore solution resistivity (ρ_o) of a concrete is influenced by the alkali contents of the cementitious materials, the mixture proportions, and the degree of hydration of the cementitious materials. It can be determined using several different methods as described in the following

section. These testing approaches are ranked based on the level of effort required with level A being the easiest, level B requiring more effort, and level C requiring the most effort. While level A testing is the easiest approach, it is the least accurate and Level C requires the most effort however it is the most accurate. The specifier should state which of these options are to be used their specification. These three approaches (Level A, B and C) are summarized below.

Level A — Assuming a Constant Pore Solution

The pore solution resistivity can be assumed to be a constant value. A value that has been suggested in previous studies is $\rho_o = 0.10\ [\Omega \cdot m]$ (31,32) based on the values of pore solution from a wide range of concretes made in several Midwestern states.

Level B — Estimate Pore Solution from the Constituents of the Chemistry

The pore solution resistivity can be estimated using a combination of mixture proportions, chemistry of the cementitious materials, and a degree of hydration. An example for this method is provided by NIST in the form of a Web application which estimates the conductive species and the volume of pore solution (33). The Web application provides the pore solution conductivity (σ_o) in units of S/m, which is the inverse of resistivity in $\Omega \cdot m$ (Equation 8):

$$\rho_o[\Omega \cdot m] = \frac{1}{\sigma_o[S/m]} \qquad \text{Equation 8}$$

Level C — Experimentally Measure Pore Solution

The pore solution resistivity can be experimentally determined using one of two methods. The first method involves extraction of the pore solution from a hardened cementitious sample (34). Specimens are placed into a high pressure die, repeatedly cycled at high pressure, and pore solution is expelled. The pore solution resistivity can be measured in a small resistivity cell (35). The second method, uses embedded sensors to measure the pore solution resistivity (36).

3.3 Measuring the Electrial Resistivity (Step 1)

While electrical methods have numerous benefits they can be significantly influenced by curing and storage conditions which can impact the degree of saturation, degree of hydration, sample temperature, and pore solution chemistry (37). To date, three sample exchanges have been conducted with several states. Sample exchanges using moist cured samples (38), sealed samples (34), and samples with embedded sensors. These sample exchanges have been used to share best practices and characterize testing variability. It has been shown that surface resistivity (AASHTO T 358-15), uniaxial resistivity (AASHTO TP 119-15), and embedded gages (39) all provide the same value for resistivity provide the samples have the same degree of hydration and conditioning and that geometry has been properly accounted for.

Recent work has indicated that determining the formation factor for a sealed concrete element has merit and should be considered for future specifications due to the simplicity associated with testing (32). The sealed sample can also be continuously monitored. To relate the sealed resistivity to the saturated resistivity, equation 9 is used (40)

$$\rho_{\ Sealed}\,[\Omega \cdot m] = \rho_{Saturated}\ [\Omega \cdot m]\ S^{-m} \qquad \text{Equation 9}$$

where ρ_{sealed} is the resistivity of a sealed sample, $\rho_{saturated}$ is the resistivity of a saturated sample and m is the saturation coefficient (a unitless number generally ranging from 3 to 5).

3.4 Summary

This section has illustrated that the time to corrosion repair can be directly related to the formation factor using Ficks second law. This has the advantage that the formation factor is a fundamental, specifiable property that can be determined using a rapid, low cost test like electrical resistivity. The approach presented has the advantage that the formation factor is performance based can be adapted to different environments, considers the geometry of the problem being investigated, and can include calculations of variability directly.

4. Example 2: Specification of Time to Critical Saturation to Assess Freeze-Thaw

4.1 Relating Degree of Saturation, Time to Critical Saturation, and Freeze-Thaw Performance

Many of the current specifications for freeze-thaw performance (SHA and ACI 318) are based on empirical observations that relate aspects of mixture design to performance. A sorption based model has been used to quantify the performance of concrete in a freeze-thaw environment (41,42) as shown in Equation 9.

$$\boldsymbol{t_{Saturation}} = \left(\frac{\boldsymbol{S_{Critical} - S_{Matrix}}}{\boldsymbol{\emptyset \dot{S}_2}}\right) \qquad \text{Equation 9}$$

Equation 9 is based on a two stage sorption process where the water absorbed after a short time fills and saturates the matrix of gel and capillary pores (S_{Matrix} represents the degree of saturation when the gel and capillary pores are filled). After these pores are saturated, the entrained and entrapped air voids begin to fill. S_2 in Equation 9 is the change in the degree of saturation as a function of the square root of time. The critical degree of saturation ($S_{Critical}$) varies as a function of air quality (43) as described in Equation 10 which was obtained as a fitted lower bound to experimental data.

$$\mathbf{S_{Critical}} = 87 - 10\ \text{SAM} \qquad \text{Equation 10}$$

A value for $S_{Critical}$ of 85% has been proposed when the quality of the air is not known. It is noted that φ (from Equation 9) can be taken as 1.0 when the concrete is in continuous contact with water. This value may be lower than 1.0 to account for drying and can be increased when deicing salt is used. Research is still needed to determine the values for φ as related to given exposure conditions.

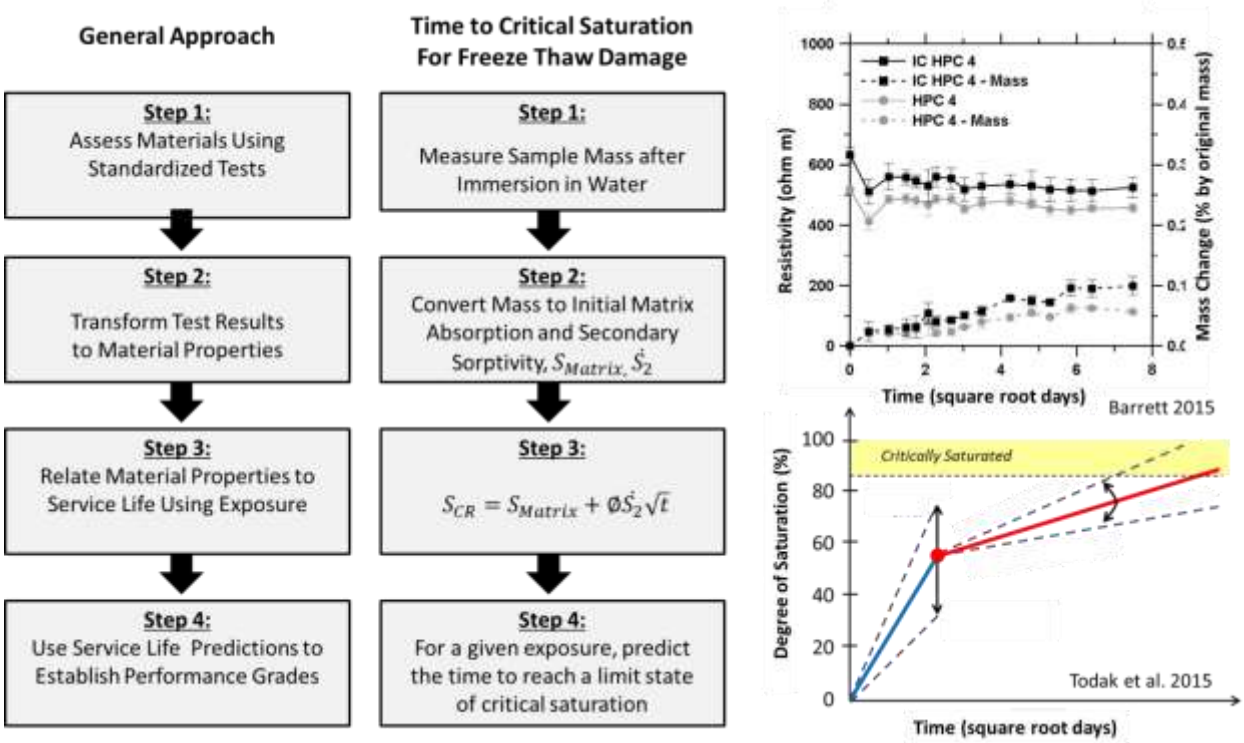

Figure 4: Extending the performance model approach to freeze-thaw damage

Thirty two samples were tested with three water to cementitious ratios (0.35, 0.40, 0.45) and a wide range of air contents and SAM numbers (44,45). An overview of results from experimentally measured durability factors as determined in accordance with ASTM C666, air content of fresh concrete, SAM numbers, and time to critical saturation are shown in Figure 5. The S_2 and S_{Matrix} was determined by a newly developed saturation test known as the "bucket test" (45).

Figure 5a plots the predicted time to reach critical saturation as a function of air content. Different symbols are used to denote the measured SAM number with filled circles noting SAM values at or above 0.20 and plus signs ("+") having a value below 0.20. Figure 5a illustrates that samples with higher air contents had a longer time to reach critical saturation. All samples with high air content (> 6.5%) exhibited a time to reach critical saturation greater than 20 years and all samples with an air content lower than 4.5% had an age to reach critical saturation that was less

than 20 years. The results for these experiments indicate that the SAM test can be used to improve the understanding the performance of concrete with an air content between 4.5 and 6.5% with samples with a SAM number less than 0.20 showing improved performance when compared with samples at the same air content.

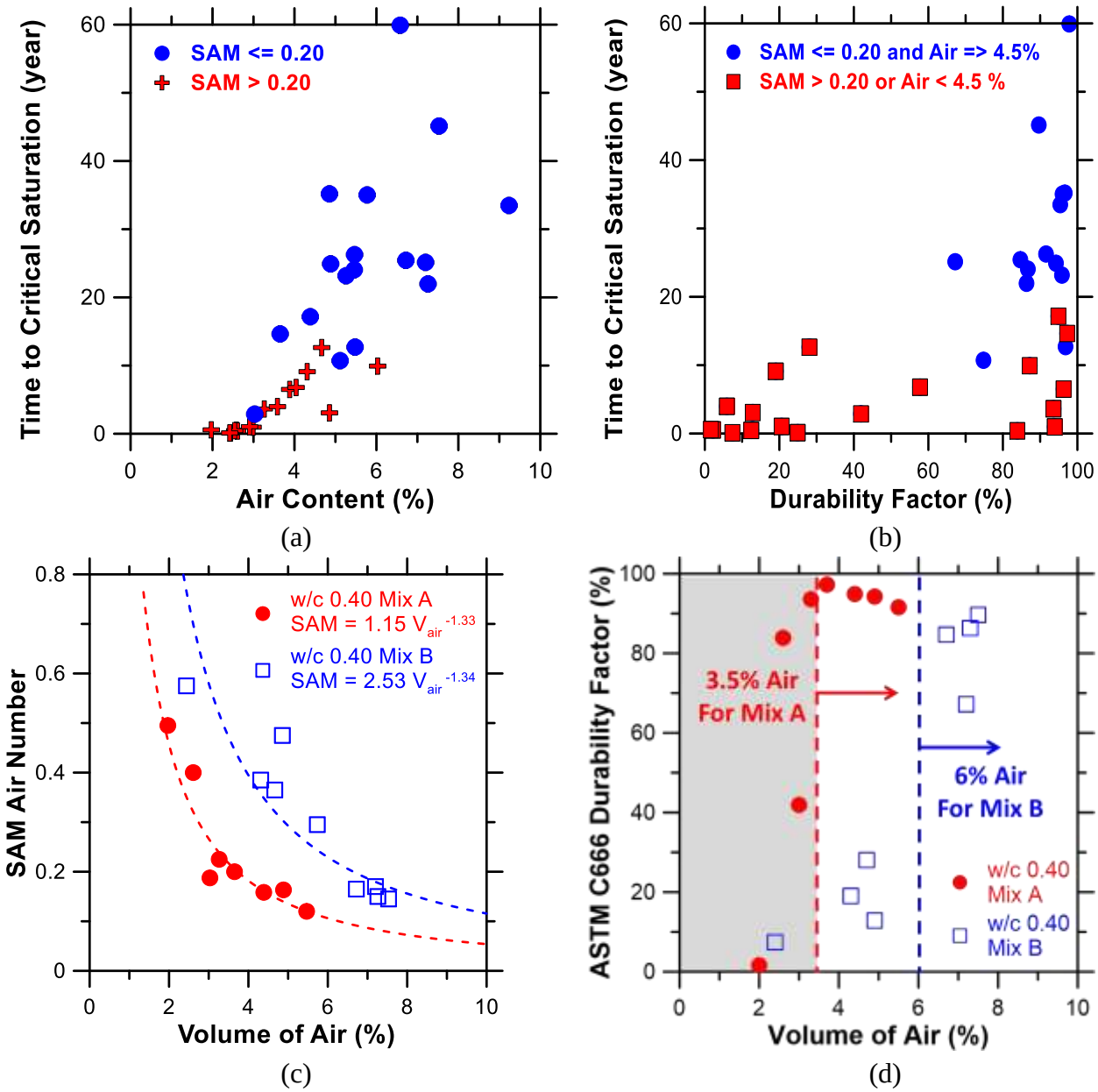

Figure 5 – The time to critical saturation for concrete: a) time to saturation versus air content, b) time to saturation versus durability factor, c) SAM air number versus the volume of air, and d) the durability factor versus air content

Figure 5b illustrates the time to reach critical saturation as a function of the durability factor as measured with ASTM C666. It can be noticed that for mixtures where the air was maintained above 4.5% and the SAM number was maintained below 0.20 the durability factor was greater than 60% at the conclusion of the test and the measured age to reach critical saturation was greater than 12 years with well over 80% of the mixtures demonstrating a service life of over 20 years even in continual contact with water.

The relationship between the air content and the SAM number is not unique and depends on the quality of the air-void system in a given concrete. Consider two concrete series made with a w/cm of 0.40 as shown in Figure 5c (44). It is observed that Mixture A has a better air-void distribution (lower SAM number) for the same total air volume. As a result, to achieve a SAM number of 0.20, a total air content of 3.7% would be needed in Mix A while an air content of 6.6% is needed for Mix B. Figure 5d illustrates the durability factor for these mixtures as measured with ASTM C666. The experimentally measured durability factor indicates that for Mixture A an air content greater than 3.5% is needed for a high durability factor while this value needs to increase to 6% for Mixture B.

Figure 6a shows the computed time to reach critical saturation for Mix A and Mix B using only Equation 9 and the experimentally measured secondary sorption (measured to be 3.4 and 4.6 %DOS/year$^{0.5}$ respectively). Figure 6 suggests that in addition to the prediction of time to saturation, an additional criteria that describes the air-void structure (e.g., SAM < 0.25) may be useful to insure long a high level of performance based on ASTM C666. Figure 6b shows the same data shown in Figure 6a, however Figure 6b only shows the time to reach crticial saturation for mixtures where a SAM air number exceeds 0.25 and the air content exceeds 4.5% (these are suggested production quality limits). When these criteria (SAM > 0.25 and Air > 4.5%) are applied, the time to reach critical saturation is predicted to be greater than 25 years for both mixtures. The implication of Figure 6b is that concrete in continuous contact with water would be expected to reach 25 years before freeze and thaw is observed which correlates with these mixtures having an ASTM C666 durability factor greater than 80%.

4.2 Measuring Degree of Saturation for Mixture Acceptance and Quality Control

While the time to reach critical saturation has benefits as it relates a concrete mixture to performance under given exposure conditions, current methods to determine the time to reach critical saturation require standardization. Current test methods like ASTM C1585 can be used to measure the rate of absorption; however they require modification to determine the degree of saturation. The research team has examined a test called the “bucket test,” which still requires standardization. The bucket test is performed by placing three concrete cylinders (cylinders that have been previously stored in a sealed condition) in a 5 gallon bucket of either lime-saturated water or a lime-saturated simulated pore solution. The mass of the sample is recorded at various

times, with the mass of the sample at 5 days being used to determine the S_{Matrix} parameter and measurements of mass between 10 and 60 days being used to determine S_2. After 60 days, the sample is oven dried and the mass is determined. The sample is vacuum-saturated and the mass again determined. It should be noted that vacuum saturation is heavily dependent on the level of vacuum drawn, and it is recommended that a vacuum of at least 50 Torr is needed to saturate a sample (46).

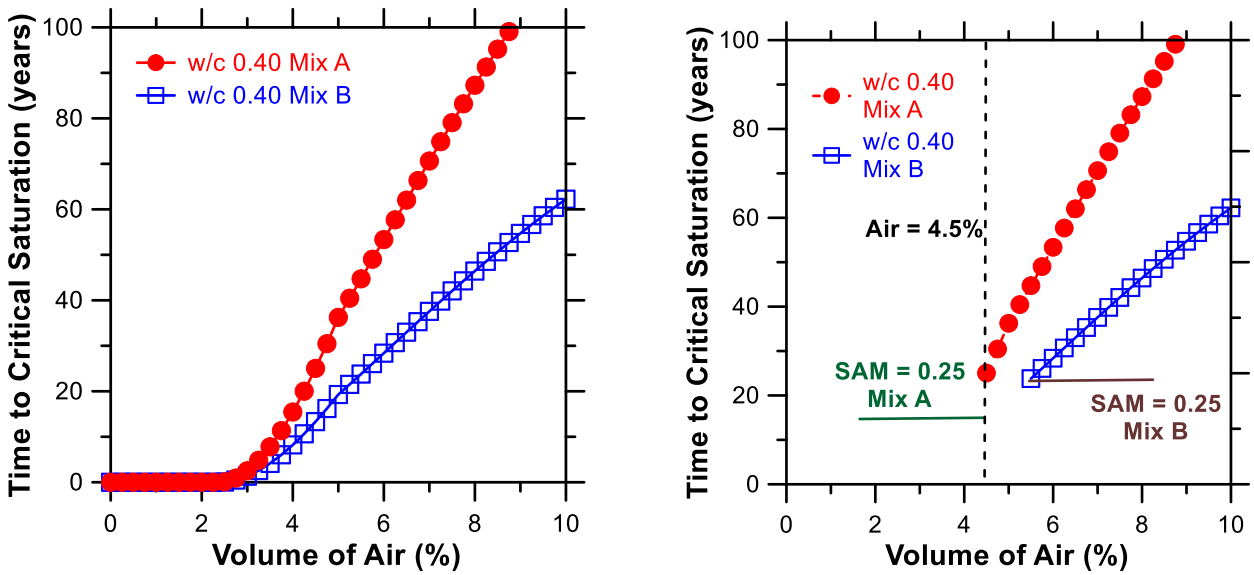

(a) *(b)*

Figure 6 – a) Time to reach critical saturation and b) time to reach critical saturation with SAM number<0.25and air greater than 4.5%

This paper has focused on freeze-thaw damage of the hydrated cement paste and has not addressed aggregate-related freeze-thaw distress (e.g. D-Cracking). This approach does not address the chemical reaction that can occur between the matrix and certain deicing salts ($MgCl_2$ and $CaCl_2$) as described elsewhere (47).

5.0 Summary

It is the premise of the authors that a performance specification can be developed for concrete durability that relates test methods, material properties, limit states and the service life of a concrete in a given environment. A framework has been provided that others can follow to help establish, validate, and extend this current effort. Two specific examples have been provided to illustrate how this framework can be applied.

First, the formation factor was used with Fick's second law to estimate chloride ingress and subsequent initiation and progression of corrosion to predict the time to repair for a

reinforced concrete structure. A procedure was shown that could determine the formation factor using electrical resistivity which can be used as a quality control method.

Second, time to critical saturation was used to predict the time to freeze-thaw damage under continuous exposure to moisture. The time to reach critical saturation was determined based on the matrix saturation, the secondary rate of sorption and the critical degree of saturation. The results show that a time to critical saturation of 25 years is consistent with a required air volume of at least 4.5% with a SAM value of at most 0.25. The total air volume, SAM number and a measure of consistency like formation factor can be used as quality control tools to demonstrate compliance with a specification.

These examples show that this approach to developing a procedure to test, predict performance, and ultimately specify concrete for durability is not only practical but possible today. This framework provides a path to illustrate how performance based specifications can evolve, tying themselves to the mechanisms of deterioration to predict the long-term performance of concrete. While additional work is needed to refine and calibrate these efforts, these promising findings should encourage SHAs that performance based specifications, based on simple tests that evaluate the mechanisms of damage, can be implemented to help them produce more durable concrete. Furthermore, these efforts can be extended other durability mechanisms.

6.0 Acknowledgements

The first author acknowledges support from “FHWA DTFH61-13-C-00025” and the first and second author acknowledge support from the pooled fund study “TP-5(297) Improving Specifications to Resist Frost Damage in Modern Concrete”. The contents of this report reflect the views of the authors. The contents do not necessarily reflect the official views or policies of a Department of Transportation or the Federal Highway Administration at the time of publication. This report does not constitute a standard, specification, or regulation

7.0 References

1 Kopac, P., “Making Roads Better and Better,” Public Roads, July/August, 2002

2 http://www.nrmca.org/sustainability/033000_final.pdf

3 Goodspeed, C. H., Vanikar, S., and Cook, R. (1996) ‘High-performance concrete defined for highway structures’ Concrete International Vol.18(2), 62-67

4 Ozyildirim, C., (1993) “High Performance Concrete for Transportation Structures," Concrete International, V. 15(1), pp. 33-38

5 Darter, M.I., Abdelrahman, M., Okamoto, P.A. and Smith, K.D., (1993) “Performance-Related Specifications for Concrete Pavements: Volume I-Development of a Prototype Performance-Related Specification”, FHWA-RD-93-042

6 Weed, R. M. “Practical Framework for Performance-Related Specifications” (1999) Transportation Research Record 1654 pp. 81-87.
7 http://www.fhwa.dot.gov/pavement/pccp/pavespec/
8 Graveen, C., Weiss, W. J., Olek, J. O., Nantung, T., and Gallivan, V. L., (2004) “Comments On The Implementation Of a Performance Related Specification (PRS) for a Concrete Pavement In Indiana,” Transportation Research Board
9 Fib Model Code for Concrete Structures 2010, (2013) Ernst and Sohn Publishers, pp. 402 ISBN 978-3-433-03061-5
10 ACI 365.1R00 “Service Life Prediction – State of the Art Report,” ACI Manual of Concrete Practice, 41 pages
11 DuraCrete/BE95-1347/R4-5 (1998) "Modelling ofDegradation", Task 2 Report.Prepared by Taywood Engineering Lirnited (TEL), United Kingdom.
12 Barde, V., Radlinska, A., Cohen, M. and Weiss, J. (2009), “Relating Material Properties to Exposure Conditions for Predicting Service Life in Concrete Bridge Decks in Indiana”, Final Report, FHWA/IN/JTRP-2007/27, Joint Transportation Research Program
13 Develop and Deploy Performance-Related Specifications (PRS) for Pavement Construction FHWA DTFH61-13-C-00025
14 Taylor, P., Ezgi, Y., Halil, C (2014) “Performance Engineered Mixtures for Concrete Pavements in the US” Civil Construction and Environmental Engineering Conference Presentations and Proceedings, Paper 24
15 Radlinska, A., and Weiss, W. J., (2012) “Toward the Development of a Performance Related Specification for Concrete Shrinkage,” ASCE Journal of Civil Engineering Materials, Vol. 23, p. 64-71
16 Shimizu, Y. An electrical method for measuring the setting time of portland cement. Mill Section of Concrete, Vol. 32, No. 5, 1928, pp 111-113.
17 Christensen, B. J., R. T. Coverdale, R. A. Olson, S. J. Ford, E. J. Garboczi, H. M. Jennings and T. O. Mason. Impedance spectroscopy of hydrating cement-based materials: measurement, interpretation, and application. Journal of the American Ceramic Society, Vol. 77, No. 11, 1994, pp 2789-2804.
18 McCarter, W. J., G. Starrs and T. M. Chrisp. Electrical conductivity, diffusion, and permeability of Portland cement-based mortars. Cement and Concrete Research, Vol. 30, No. 9, 2000, pp 1395-1400.
19 Rupnow, T., Icenogle, P., (2012) “Evaluation of Surface Resistivity Measurements as an Alternative to the Rapid Chloride Permeability Test for Quality Assurance”, Transportation Research Board
20 Gudimettla, J. M., Crawford, G. L., (2014) “Field Experience in Using Resistivity Testgs for Concrete,” Transportation Research Board http://docs.trb.org/prp/15-3357.pdf
21 Morris, W., E. I. Moreno and A. A. Sagues. Practical evaluation of resistivity of concrete in test cylinders using a Wenner array probe. Cement and Concrete Research, Vol. 26, No. 12, 1996, pp 1779-1787.
22 Bentur, A., Berke, N., and Diamond, S., (1997) “Steel Corrosion in Concrete: Fundamentals and Civil Engineering Practice,” CRC Press, 208 pages
23 Isgor, O.B., Razaqpur, A.G, 2006, "Modelling steel corrosion in concrete structures," Materials and Structures, 39(3): 291-302

24 Ghods, P. Isgor, O.B., Pour-Ghaz, M. 2007, "A practical method for calculating the corrosion rate of uniformly depassivated reinforcing bars in concrete, Materials and Corrosion, 58(4): 265-272
25 Isgor, O.B., Razaqpur, A.G, 2006, "Modelling steel corrosion in concrete structures," Materials and Structures, 39(3):291-302
26 Azad, V.J., Isgor, O.B., 2016, "Thermodynamic perspective on admixed chloride limits of concrete produced with SCMs," ACI Special Publication (SP-308), pp. 1-18
27 Resistance of Concrete to Chloride Ingress – Testing and Modelling. Taylor & Francis Group Ltd, Oxford 2011 (Tang Luping, L-O Nilsson, Muhammed Basheer)
28 Bu, Y., Luo, D., and Weiss, W.J., (2015), "Using Fick's Second Law and the Nernst-Planck Approach in the Prediction of Chloride Ingress in Concrete Materials," Advances in Civil Engineering Materials Advances in Civil Engineering 01/2015; 2015:1-13. DOI:10.1155/2015/929864
29 Hooton, R.D., (2008) 'Bridging the gap between research and standards', Cement and Concrete Research, Volume 38, Issue 2, February 2008, Pages 247-258
30 Paredes, M., N. M. Jackson, A. El Safty, J. Dryden, J. Joson, H. Lerma and J. Hersey. Precision Statements for the Surface Resistivity of Water Cured Concrete Cylinders in the Laboratory. Advances in Civil Engineering Materials, Vol. 1(1), 2012
31 Coyle, A., Spragg, R., Amirkhanian, A., Weiss, W. J., (2016) "Measuring the Influence of Temperature on Electrical Properties of Concrete," International RILEM Conference on Materials Systems and Structures in Civil Engineering Conference Segment on Service Life, August 22-24, 2016 Lyngby
32 Weiss, W.J., Barrett, T.J., Qiao, C., and Todak, H., (2016) "Toward A Specification for Transport Properties of Concrete Based on the Formation Factor of A Sealed Specimen," Advances in Civil Engineering Materials,
33 Bentz, D. P. A virtual rapid chloride permeability test. Cement and Concrete Composites, Vol. 29, No. 10, 2007, pp. 723–731
34 Barneyback, R. S., and Diamond, S., "Expression and analysis of pore fluids from hardened cement pastes and mortars," Cement and Concrete Research, Volume 11, Issue 2, March 1981, Pages 279-28
35 Spragg, R., and Weiss, W. J., (2016) "Chapter 11: Assessing a concrete's resistance to chloride ion ingress using the formation factor," Corrosion of Steel in Concrete Structures, 1st Edition
36 F. Rajabipour, J. Weiss, 'Material Health Monitoring of Concrete by Means of Insitu Electrical Conductivity Measurements', Cement Wapno Beton, 2 (March 2007) 76-92
37 Spragg, R., Villani, C., Snyder, K., Bentz, D. P., Bullard, J. W., and Weiss, W. J., (2013) "Electrical Resistivity Measurements in Cementitious Systems: Observations of Factors that Influence the Measurements," Transportation Research Record
38 Spragg, R., Castro, J., Nantung, T., Paredes, M., and Weiss, W. J., (2012) "Variability Analysis of the Bulk Resistivity of Concrete Measured Using Cylinders," ASTM – Advances in Civil Engineering Materials, Vol. 1, No. 1, p. 17 10.1520/ACEM104596
39 Poursaee, A., and Weiss, W. J., (2010) "An Automated Electrical Monitoring System (AEMS) to Assess Concrete Property Development, Journal of Automation in Construction, Volume 19, Issue 4, July 2010, Pages 485-490

40 Weiss, J., Snyder, K., Bullard, J., and Bentz, D. (2013). "Using a Saturation Function to Interpret the Electrical Properties of Partially Saturated Concrete." J. Mater. Civ. Eng., 10.1061/(ASCE)MT.1943-5533.0000549, 1097-1106.
41 G. Fagerlund, “The long-time water absorption in the air-pore structure of concrete,” 1993
42 Weiss, W. J., Tsui-Chang, M., and Todak, H., (2016) “Is the Concrete Profession Ready for Performance Specifications that Provide an Alternative to Prescriptive W/C and Air Content Requirements, National Ready Mixed Concrete Association Annual Meeting, Washington DC
43 AASHTO TP 118 (2015) Standard Method of Test for Characterization of the Air-Void System of Freshly Mixed Concrete by the Sequential Pressure Method
44 Improving Specifications to Resist Frost Damage in Modern Concrete Mixtures, Led by Tyler Ley, Oklahoma DOT
45 Todak, H., (2015) “Durability Assessments of Concrete using Electrical Properties and Acoustic Emission Testing,” MSCE Thesis, Purdue University
46 Bu, Y., Spragg, R., and Weiss, W. J. "Comparison of the Pore Volume in Concrete as Determined Using ASTM C642 and Vacuum Saturation," *Advances in Civil Engineering Materials*, Vol. 3, No. 1, 2014, pp. 308-315
47 Suraneni, P., Azad, V. J., Isgor, B. O., and Weiss, W. J., (2016) “Deicing Slats and Durability of Concrete Pavement Joints: Mitigating Calcium Oxychloride Formation”, Concrete International, vol. 38., Issue 4, April 2016